energies

MDPI

Article

Energy Harvesting Based on a Novel Piezoelectric $0.7PbZn_{0.3}Ti_{0.7}O_3$-$0.3Na_2TiO_3$ Nanogenerator

Zainab Radeef [1,2,*], Chong Wen Tong [1], Ong Zhi Chao [1,3] and Khoo Shin Yee [1,3,*]

1 Department of Mechanical Engineering, Faculty of Engineering, University of Malaya, 50603 Kuala Lumpur, Malaysia; chong_wentong@um.edu.my (C.W.T.); alexongzc@um.edu.my (O.Z.C.)
2 Department of Material, Faculty of Engineering, University of Kufa, 31001 Al Najaf, Iraq
3 Advanced Shock and Vibration Research Group, Applied Vibration Laboratory, Block R, Faculty of Engineering, University of Malaya, 50603 Kuala Lumpur, Malaysia
* Correspondence: zina_engi@siswa.um.edu.my (Z.R.); mikeson.khoo@yahoo.com or khooshinyee@um.edu.my (K.S.Y.)

Academic Editor: K.T. Chau
Received: 21 January 2017; Accepted: 2 May 2017; Published: 6 May 2017

Abstract: Recently, piezoelectric materials have achieved remarkable attention for charging wireless sensor nodes. Among piezoelectric materials, non-ferroelectric materials are more cost effective because they can be prepared without a polarization process. In this study, a non-ferroelectric nanogenerator was manufactured from $0.7PbZn_{0.3}Ti_{0.7}O_3$-$0.3Na_2TiO_3$ (PZnT-NT). It was demonstrated that the increment of conductivity via adding the Na_2TiO_3 plays an essential role in increasing the permittivity of the non-ferroelectric nanogenerator and hence improved the generated power density. The dielectric measurements of this material demonstrated high conductivity that quenched the polarization phase. The performance of the device was studied experimentally over a cantilever test rig; the vibrating cantilever (0.4 ms^{-2}) was excited by a motor operated at 30 Hz. The generated power successfully illuminated a light emitting diode (LED). The PZnT-NT nanogenerator produced a volume power density of 0.10 $\mu w/mm^3$ and a surface power density of 10 $\mu w/cm^2$. The performance of the proposed device with a size of ($20 \times 15 \times 1$ mm^3) was higher in terms of power output than that of the commercial microfiber composite (MFC) ($80 \times 57 \times 0.335$ mm^3) and piezoelectric bimorph device ($70 \times 50 \times 0.7$ mm^3). Compared to other existing ferroelectric and non-ferroelectric nanogenerators, the proposed device demonstrated great performance in harvesting the energy at low acceleration and in a low frequency environment.

Keywords: conductivity; energy harvesting; ferroelectric; nanogenerator; permittivity; piezoelectric

1. Introduction

The conversion of wasted mechanical vibration to useful electrical energy is one of the underlying strategic issues in the field of sustainable energy. Due to their high sensitivity to surrounding vibrations, piezoelectric materials have been employed through different techniques and manufacturing processes to this end.

Commercial piezoelectric materials can be classified into single crystal, soft piezoelectric, hard piezoelectric [1], piezo-polymer composite groups, and nanogenerator. The common conventional methods of piezoelectric material preparation are the solid–state method [2,3] and wet chemical methods such as the hydrothermal method and the solution gel (Sol–Gel) method [4]. Wet chemical methods are carried out at lower temperatures and hence became more attractive, especially for the nanogenerator harvesters.

The nanogenerator could be classified by ferroelectric and non-ferroelectric materials. Recent studies have demonstrated that high power density could be harvested from vibration

energies using both ferroelectric and non-ferroelectric nanogenerators [5–10]. It is well known that the ferroelectric material and the perovskite structure are utilized immensely in the energy harvesting field due to the high piezoelectric strain constant, high remnant polarization, and high permittivity [11]. Silicon nanowires (SiNWs) are an example of ferroelectric nanogenerators that are normally covered by a thin flexible polymer, and the importance of preventing the short current leakage in SiNWs is highlighted in [10], in order to improve the harvesting performance. Another enhancement of a nanogenerator can be achieved by using pre-treatment processes, such as reducing oxygen vacancies, air annealing, applying Schottky contact techniques, and increasing the conductivity.

In fact, non-ferroelectric materials have low electromechanical properties (such as low piezoelectric strain constant and low permittivity). However, such films can be prepared without a polarization process, making them cost effective in the industry. Thus, studies have shifted towards investigating the fabrication of non-ferroelectric nanogenerators. Previous studies demonstrated that non-ferroelectric nanogenerators or nanogenerators with low ferroelectric phase materials can provide high current density (close circuit). Thus, it has a great competitive advantage compared to the brittle lead zirconate titanate (PZT) piezoelectric ferroelectric harvesters. In this regard, the non-ferroelectric zinc oxide nanogenerator (ZnO-NG) has achieved rapid progress and has become an aggressive competitor regarding ferroelectric materials in the energy harvesting field [12–14], and such material has high power density and comparable current density [7,12–20].

The commonly used ZnO-NG has a systematically aligned nanowire [7,13,21] where it could provide enough power for illuminating light emitting diodes (LEDs) or liquid crystal display (LCD) screens [7]. Overall, the flexible ZnO-NG provides higher power density compared with other flexible ferroelectric harvesters [6,10,12–14,22,23]. The figures of merit of ZnO-NG was studied by Hinchet [24], where high vibration harvesting performance can been achieved via long and thin nanowires.

Generally, a ferroelectric material is polarized under a high electric field where the random orientation of the dipoles will be aligned permanently. Hence, the material gains permanent polarization. In this way, the polarized material has a distinct high response and it has the capability to generate a high pulsing amplitude. The ferroelectric harvesters exhibit very high voltages (open circuit) whereas the non-ferroelectric harvesters can generate a high current density [14,18,20].

In this regard, the ferroelectric phase of $PbZnTiO_3$ will be evaluated in this study due to the fact that there are inadequate estimations or studies of such types of piezoelectric materials. Accordingly, the material will be mixed with ion exchange media, and the alteration of its physical properties will be implemented by using nano-alkaline titanate for employing it as an energy harvester. $PbZnTiO_3$ has been employed for sensing applications and utilized as a memory storage device [25,26]. The nano-alkaline material used in this study is sodium titanate, Na_2TiO_3 (NT), which is commonly utilized in numerous applications such as ion exchange media and potential proton conduction of fuel cells [27]. In fact, $PbZnTiO_3$ is a ferroelectric material [28] while NT provides good conductive properties. Normally, the conductivity affects the ferroelectric behavior. Thus, the weight ratio of the NT is a vital issue that characterizes the ferroelectric phase of the harvester, whereas using a too high weight ratio from such conductive fillers could cause polarization quenching [29]. The power density, maximum voltage (open circuit,) and current (short circuit) were studied here.

Recently, the enhancement of the piezoelectric strain and permittivity has been achieved by adding supplement conductive fillers such as nano-carbon, nano-carbon black [25,26], and nano-graphite [27,28]. Sufficient volume fractions of such conductive fillers enhances the poling efficiency of the ferroelectric materials [29]; however, an excessive amount of the conductive filler ratio yields a reduction of the ferroelectric phase.

In fact, the optimal supplied power can be achieved only when the piezoelectric impedance matches with the load impedance, where there is a drop in electrical loss and an increase of the power transfer amount. In accordance with that, the impedance will be compared for various examined harvesters (i.e., PZT, microfiber composite (MFC) and $0.7PbZn_{0.3}Ti_{0.7}O_3$-$0.3Na_2TiO_3$ (PZnT-NT)) in this study.

The designed harvester consisted of a PZnT-NT nanogenerator, which was compacted by two stiff electrodes (i.e., copper and zinc electrodes) for resisting deterioration. In this paper, the fabrication procedure, characterization, and the conductivity influence of PZnT-NT were studied. Finally, the power density was recorded and compared with two common types of piezoelectric harvesters.

2. Theory

An energy harvesting device has been fabricated from the PZnT-NT system. The constructed device characterized the effect of the ratio of Na_2TiO_3, and the performance of the device is examined using a cantilever beam system, where the performance of PZnT-NT is compared with flexible and brittle PZT harvesters. The dielectric constant, loss tangent, and conductivity have been studied. The dielectric constant or permittivity constant is denoted by K_3^T and it can be expressed by the permittivity of the material (ε_T) per permittivity in a vacuum (ε_O = 8.854 × 10^{-12} F.m^{-1}), Also, we can calculate the relative permittivity from the real dielectric part (ε') and the imaginary part (ε''), as shown in Equation (1):

$$K_3^T = \frac{\varepsilon_T}{\varepsilon_o} = \varepsilon' - j\varepsilon'' \quad (1)$$

The dielectric loss tangent, tan (δ), is defined as the ratio between the loss energy to the stored energy in the medium, where there is a portion of electromagnetic energy that will be dissipated as heat under an alternating electric field:

$$\tan(\delta) = \frac{\varepsilon''}{\varepsilon'} \quad (2)$$

The AC conductivity, σ, can be computed as follows:

$$\sigma = \omega\varepsilon'\varepsilon_o tan(\delta) \quad (3)$$

where ω is known as the angular frequency ($2\pi f$).

Finally, the storing energy E_C is computed by multiplying the capacitance of the external capacitor and the accumulated voltage, as expressed in Equation (4):

$$E_C = \frac{1}{2} C_C V_t^2 \quad (4)$$

where C_C is the external capacitor and V_t is the voltage in the steady state.

The power generation or the dissipated power of the load, P, across the applied resistances, is computed as follows:

$$P = \frac{V^2}{R_L} \quad (5)$$

where V is the voltage at the steady state and R_L is the load resistance of the rectifier circuit. The challenge in energy harvesting is the harvesting of energy under low frequencies, low acceleration, and strain. This requires using a soft doped piezoelectric material or using thin films. This research sought to fabricate a sustainable nanoparticle piezo-harvester with lower cost and higher performance.

The typical power provided by the flexible MFC film ranges between 4 mJ/s and 13 mJ/s at 10 Hz excitation with an acceleration of 1 G, and strain of 800 ppm [30]. In these studies, MFC chips were employed for comparing and evaluating the power outputs; MFC is characterized by high piezoelectric coefficients (d_{33}), high permittivity (ε), high dielectric losses, and low mechanical quality factors [31–33]. The typical properties of MFC and PZT-5H are provided in Table 1.

Table 1. The electromechanical properties of the harvester. MFC: microfiber composite.

Material	MFC (MFC-PZT5A1, M8557P2)	Piezoelectric Bimorph (PZT-5H)
Typical capacitance (nF)	325	184
Piezoelectric strain constant, d_{33} (pC/N)	470	600
Piezoelectric voltage constant, g_{33} (10^{-3} Vm/N)	25	19.4
Permittivity, $\frac{\varepsilon^T_{33}}{\varepsilon_O}$ (at 1 kHz)	1300	3500
Electrode material and configuration	Flexible MFC with gold electrodes	Rigid Bimorph with copper-silver electrodes
Dimension (mm^3)	80 × 57 × 0.335	70 × 50 × 0.7

3. Preparation of the $0.7PbZn_{0.3}Ti_{0.7}O_3$-$0.3Na_2TiO_3$ Harvester

The piezoelectric nanogenerator was fabricated from a $0.7PbZn_{0.3}Ti_{0.7}O_3$-$0.3Na_2TiO_3$ (PZnT-NT) system. The $PbZn_{0.3}Ti_{0.7}O_3$ powder was fabricated from lead oxide (99.5% purity, R&M Marketing, Essex, UK), titanium dioxide (99.5% purity, R&M Marketing, Essex, UK) and zinc oxide (>99.0–100.5% purity, R&M Marketing. Essex, UK). The $PZn_{0.3}Ti_{0.7}O_3$ was prepared with a 1:1 stoichiometry, where the powder was calcined at 850 °C for 3 h with a heating/cooling rate of 5 °C/min. The powder was mixed by ball milling for 1 h. Sodium titanate were synthesized with a molar stoichiometry of ($NaOH:TiO_2$, 2:1) and was mixed with $0.7PbZn_{0.3}Ti_{0.7}O_3$ powder by spraying distilled water to increase the solubility. Furthermore, the particle binding was increased through the pressing process, where the sample was pressed at 3 tons. Then, the compound was deposited between two electrodes, which consisted of a copper (80 µm) anode and zinc (420 µm) cathode, and the compound was treated at 250 °C for 30 min. Finally, the electrodes were covered by high adhesive plastic tape for a hermetic covering to provide protection against environmental damage. Field emission scanning electron microscope (FESEM) image analysis was carried out to explore the surface characteristics. The physical properties of the harvester have been measured by using a precision impedance analyser (model 4294A) where the capacitance, dielectric constant, loss tangent, and conductivity have been recorded and studied based on the polarized phase of the material. The powder had been examined by an X-ray diffraction system (PANalytical X'Pert^3 X-ray diffractometer) using anode material copper (Cu), 40 mA, 40 kV, and the microstructure of the propertied PZnT-NT system was observed by FESEM image analysis. The fabricated harvester is illustrated in Figure 1.

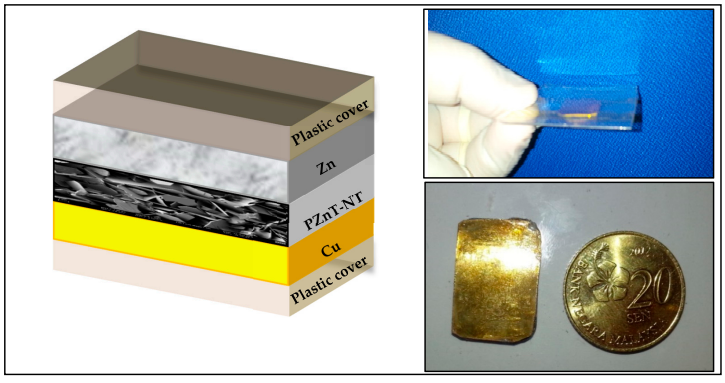

Figure 1. The piezoelectric harvester made of $0.7PbZn_{0.3}Ti_{0.7}O_3$-$0.3Na_2TiO_3$ (PZnT-NT).

Characterization of the PZnT-NT Harvester

Herein the crystallographic details of the PZnT-NT are described. The $PbZn_{0.3}Ti_{0.7}O_3$ comprises two crystalline phase, i.e., tetragonal and hexagonal with space groups of P4mm and P63mc, respectively. The tetragonal crystal lattice is a (Å) 3.9, b (Å) 3.9, and c (Å) 4.0, and the lattice angles (Alpha = Beta = Gamma) are 90°. The hexagonal crystal lattice is a (Å) 3.2, b (Å) 3.2, and c (Å) 5.2 and

the lattice angles (Alpha = Beta ≠ Gamma) are 90°, 90°, and 120°, respectively. In fact, the hexagonal crystal lattice comes from the presence of zinc oxide. The crystal system of Na_2TiO_3 is tetragonal and the space group is I41/mad. The crystal lattice is a (Å) 3.7, b (Å) 3.7, and c (Å) 9.5, and the lattice angles (Alpha = Beta = Gamma) are 90°, as shown in Figure 2.

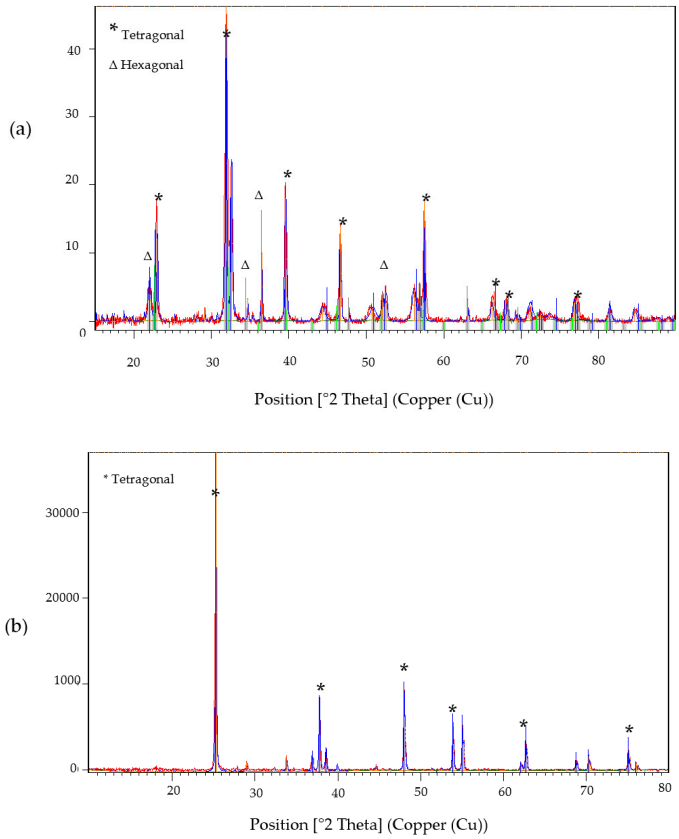

Figure 2. XRD patterns of $0.7PbZn_{0.3}Ti_{0.7}O_3$-$0.3Na_2TiO_3$: (**a**) $PbZn_{0.3}Ti_{0.7}O_3$; and (**b**) Na_2TiO_3.

The FESEM microscope image demonstrates the fabricated $0.7PbZn_{0.3}Ti_{0.7}O_3$-$0.3Na_2TiO_3$, where the system consists of $PbZn_{0.3}Ti_{0.7}O_3$ and sodium titanate nanosheets, as illustrated in Figure 3.

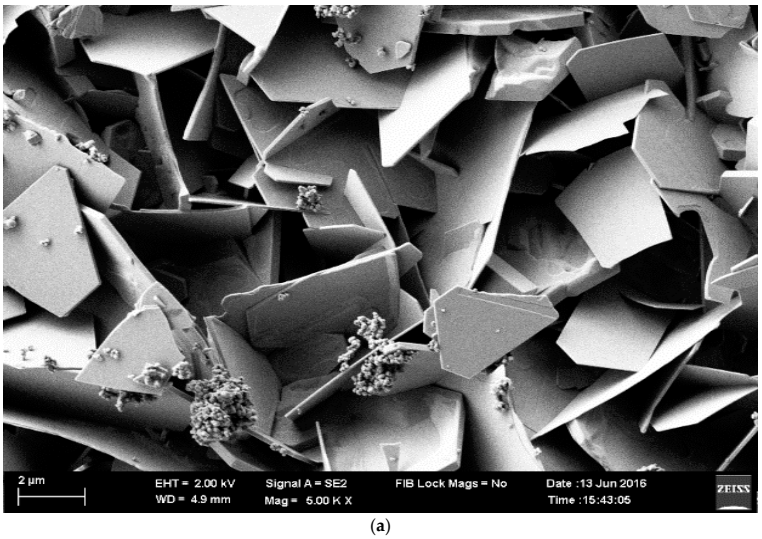

(**a**)

Figure 3. *Cont.*

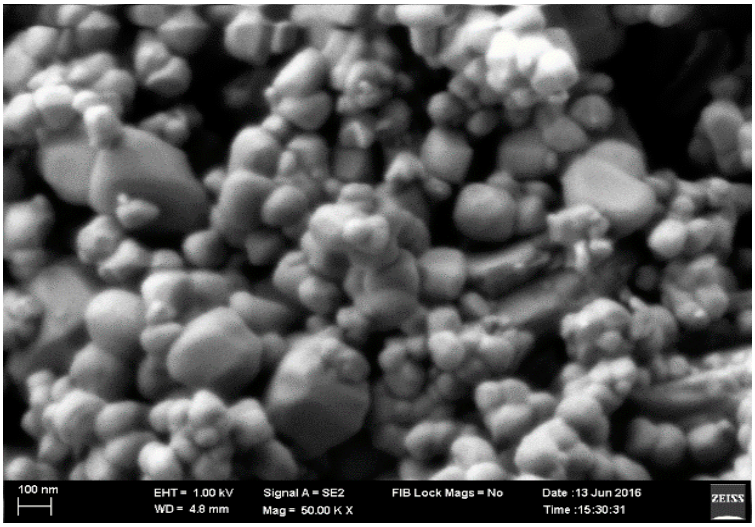

(**b**)

Figure 3. Surface characteristics of (**a**) sodium titanate (Na_2TiO_3) sheets; (**b**) $PbZn_{0.3}Ti_{0.7}O_3$ nanoparticles.

The piezoelectric dielectric constant was characterized by using an impedance analyser from 4 Hz to 110 MHz, where PZnT-NT demonstrated a high dielectric constant. Figure 4 presents the variation between PZnT-NT and the pure $PbZn_{0.3}Ti_{0.7}O_3$. Indeed, the sodium titanate sheets have the essential role of increasing the conductivity between the composite particles. A high variation in relative permittivity between the PZnT-NT and the pure $PbZn_{0.3}Ti_{0.7}O_3$ has been observed below the frequency of 5 kHz, where the permittivity of PZnT-NT decreases intensely with increasing frequency.

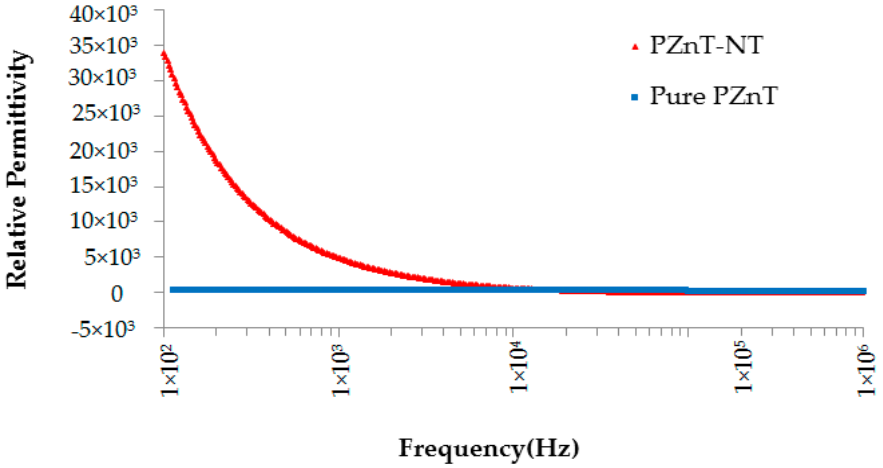

Figure 4. The dielectric properties of PZnT-NT.

The PZnT-NT yields a high loss tangent of 3.84 at 1 kHz, while the pure $PbZn_{0.3}Ti_{0.7}O_3$ produces a very low loss tangent (i.e., 0.122) due to the fact that both the stored energy and dissipated energy are low. The maximum loss tangent is 4.89 at a frequency of 5.5 kHz, where below this level the storage energy is higher than the dissipated energy. This fact is illustrated in Figure 5.

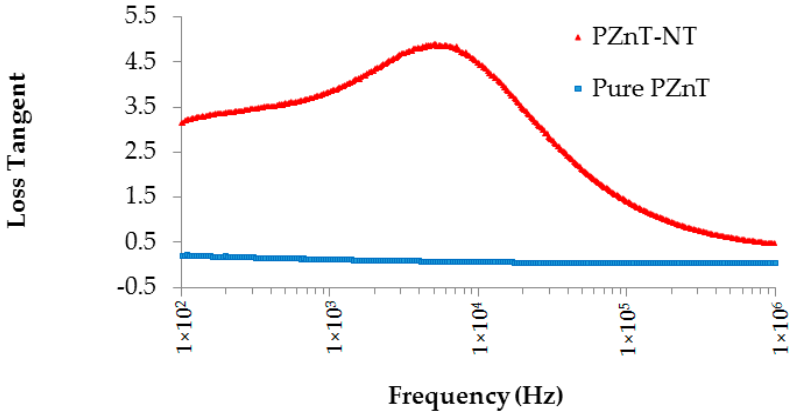

Figure 5. Loss tangent of PZnT-NT.

The conductivity of PZnT-NT and pure $PbZn_{0.3}Ti_{0.7}O_3$ has been provided in Figure 6. It is observed that the conductivity increased by adding the Na_2TiO_3 material. The material has a high dissipation of energy, due to the damping of the dipole moment and the influence of the conductive filler. The electrical conductivity (σ_e) of the PZnT-NT, the pure $PbZn_{0.3}Ti_{0.7}O_3$, and the raw Na_2TiO_3 (0% PZnT) are 3.76 $\times$ 10^{-4} S/m, 2.88 $\times 10^{-6}$ S/m, and 1.15 $\times$ 10^{-3} S/m, respectively, under room temperature and at a frequency of 1 kHz.

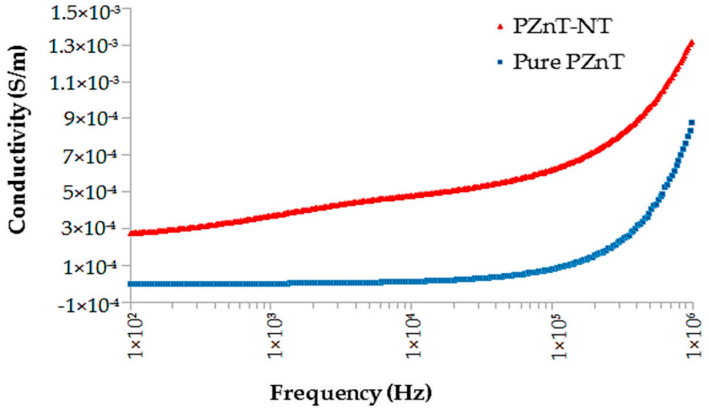

Figure 6. Conductivity of the PZnT-NT and the pure $PbZn_{0.3}Ti_{0.7}O_3$ at room temperature.

Figure 7 illustrates the hysteresis loops of the $PbZn_{0.3}Ti_{0.7}O_3$ that was sintered at 850 °C. It was observed that the material exhibited a ferroelectric behavior. The $PbZn_{0.3}Ti_{0.7}O_3$ produced a low remnant polarization (P_r) of 1.09 μC/cm^2 under an electric field of 7 kV/cm. It is worthwhile to mention that in recent advances, the highest remnant polarization of ferroelectric materials has reached 62 μC/cm^2 in piezoelectric ferroelectric materials [34]. As a consequence, the low remnant polarization is an indicator of the low response of the $PbZn_{0.3}Ti_{0.7}O_3$ and the forward shift quenches the polarity that can lead to enhancing the performance. In this study, the hysteresis loop of $0.7PbZn_{0.3}Ti_{0.7}O_3$-$0.3Na_2TiO_3$ is unable to be obtained under high voltage up to 1 kV/cm due to the conductivity. Thus, the reduction of the percentage of the conductive filler (i.e., perform the hysteresis loop test for the $0.9PbZn_{0.3}Ti_{0.7}O_3$-$0.1Na_2TiO_3$ material instead of the $0.7PbZn_{0.3}Ti_{0.7}O_3$-$0.3Na_2TiO_3$ material) has been implemented. The recorded results of the poled $0.9PbZn_{0.3}Ti_{0.7}O_3$-$0.1Na_2TiO_3$ show a reduction of the ferroelectric property, and the remnant polarization and field strength were 0.006 μC/cm^2 and 1 kV/cm, respectively. Overall, the results show that the dielectric property (relative permittivity) of the proposed PZnT-NT nanogenerator can be enhanced by adding conductive filler material. This will eventually enhance the generated power density.

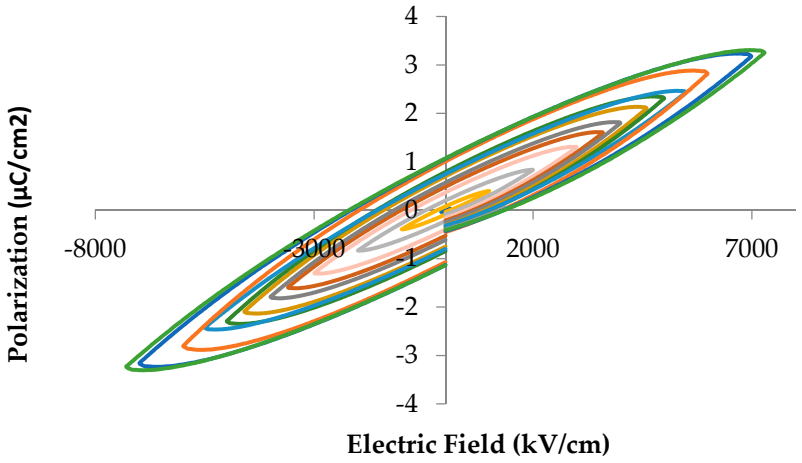

Figure 7. Hysteresis loop of pure $PbZn_{0.3}Ti_{0.7}O_3$ versus various applied electric fields.

4. Energy Harvesting and the Experimental Setup

The energy harvesting test procedure was carried out by fixing the piezoelectric harvesters directly above the host cantilever test rig, which was excited to produce a cyclic excitation at a low excitation frequency (i.e., 30 Hz) and at a low acceleration (i.e., 0.4 ms^{-2}). The generated power was compared with other commercial piezoelectric harvesters, such as MFC and PZT bimorphs. All the vibration data were measured by an accelerometer (model: SNAP S100C) through a data acquisition unit (Model: NI USB-9162, National Instruments Corporation, North Mopac Expressway, Austin, TX, USA). Hence, data were analysed by using virtual instrument software (i.e., DASYLab (Version 10, Measurement Computing Corporation, Norton, MA, USA)), and the acquired information was the frequency, acceleration, and generated voltage. The experimental setup is shown in Figure 8.

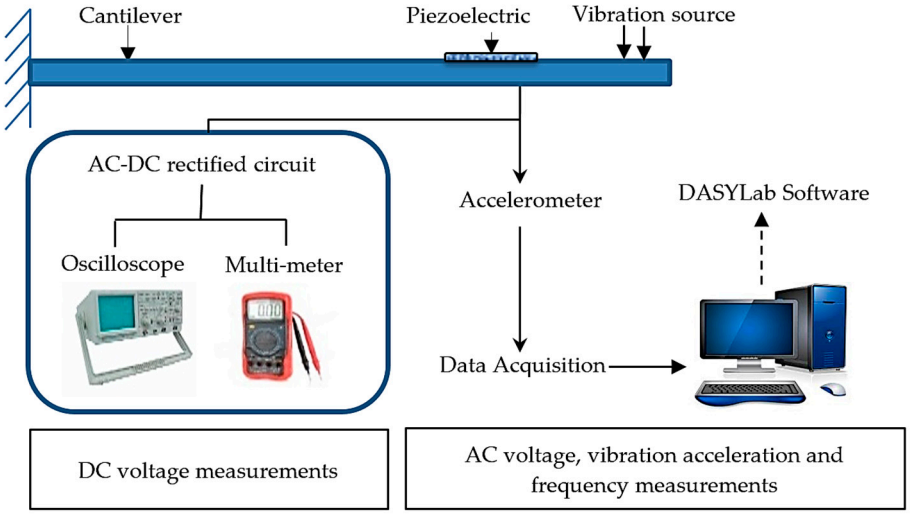

Figure 8. Energy harvesting experimental setup.

To achieve full-wave rectification, the AC voltage generated by the vibration harvester should be rectified by using a voltage regulator circuit. The AC-DC converter consists of four Schottky diode bridges (1N5817). An oscilloscope (SS5702) and multi-meter (model ZELM05 ATEX 0274) were employed for measuring the DC voltage across the capacitor and the load resistance. Maximum harvesting energy was verified when the internal impedance of the piezoelectric material matches the applied load resistance.

5. Results and Discussion

In our initial investigation, the ability of the proposed harvester to power LEDs (5 mm) at frequencies up to 10 Hz was an indicator of the optimized performance that was realized under such low frequency and acceleration rates. Figure 9 illustrates the illuminated LEDs. In this study, all the harvesters (PZnT-NT, PZT bimorph, and MFC) have been examined under the excitation frequency of 30 Hz and acceleration response of 0.4 m/s^2. The comparison of the harvesters' performances such as voltage generation, current, and power density are reported as follows.

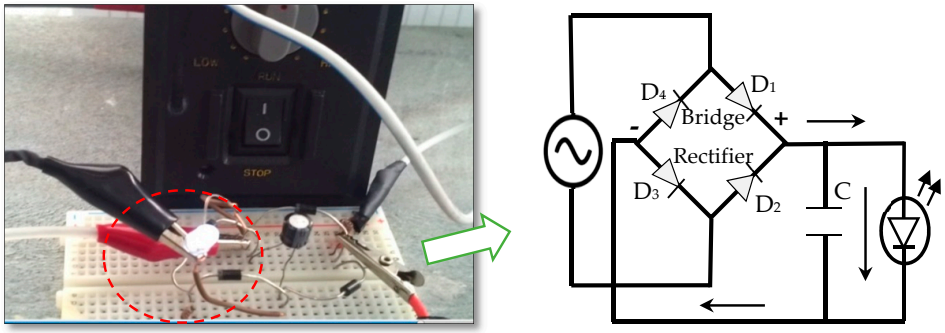

Figure 9. Flashing up light emitting diode (LED) (5 mm).

The voltage was recorded across a range of resistances between 1.9 kΩ and 5.2 MΩ. The performance of the PZnT-NT was compared with the MFC and PZT bimorphs, and the results show an outstanding performance of the PZnT-NT in spite of its insignificant size. There are increases in the voltage (V) with the increase of resistance (R_L). Furthermore, it is found that the PZnT-NT and MFC generate the highest voltages of 5.27 V and 3.34 V at a load resistance of 1908 kΩ, respectively, whereas the highest voltage of the PZT bimorph was 3.3 V at a load resistance of 2900 kΩ; this fact is illustrated in Figure 10.

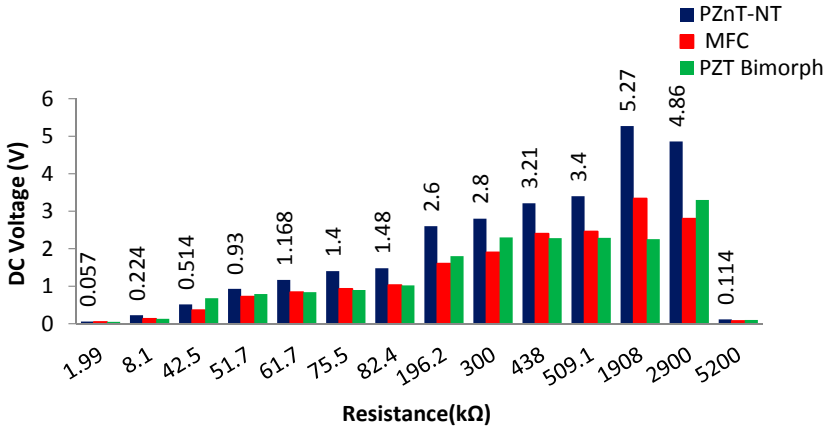

Figure 10. The generated voltage at a frequency of 30 Hz of various harvesters.

Consequently, the dissipated power was recorded across the full wave of the rectifying circuit; the maximum power was verified when a circuit load matched the impedance of the transducer. At the optimal load and steady state conditions, the stored energy of the capacitor that was supplied by PZnT-NT, MFC and PZT bimorphs was 0.34 mJ, 0.139 mJ, and 0.136 mJ, respectively. The optimal power of the PZnT-NT was verified at the load resistance of 196.2 kΩ as 0.03 mW. The optimal power of the MFC and PZT bimorphs were 0.0189 mW and 0.0176 mW with the corresponding loads of 438 kΩ and 300 kΩ, respectively, as illustrated in Figure 11.

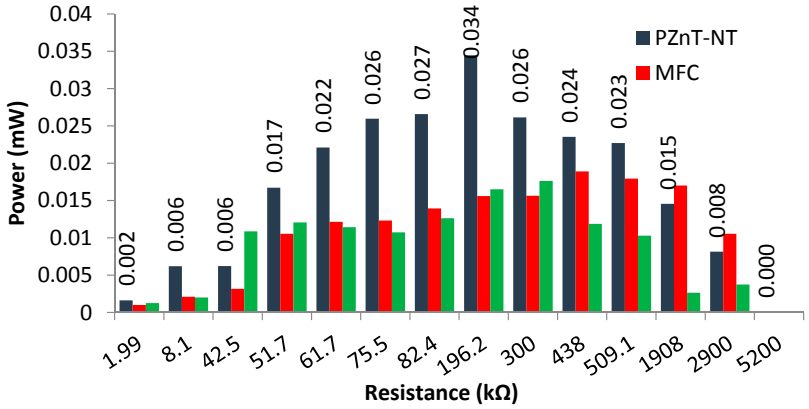

Figure 11. Optimal power output of various harvesters.

The variations between the generated currents for PZnT-NT, and MFC and PZT bimorphs are illustrated in Figure 12. The maximum DC current exhibited by the PZnT-NT and PZT bimorph was comparable at the range where the MFC generated the lowest current. The maximum DC current was recorded for the PZnT-NT, and the MFC and PZT bimorphs at the optimal applied loads and were 0.0133 mA, 0.0055 mA, and 0.007 mA, respectively. By considering the harvester's size, the power densities of various types of harvesters have been computed and are shown in Figure 13. The results affirmed that the PZnT-NT harvester produces the highest power density (i.e., 0.13 $\mu w/mm^3$), compared to the MFC (i.e., 0.014 $\mu w/mm^3$) and PZT bimorphs (i.e., 0.007 $\mu w/mm^3$).

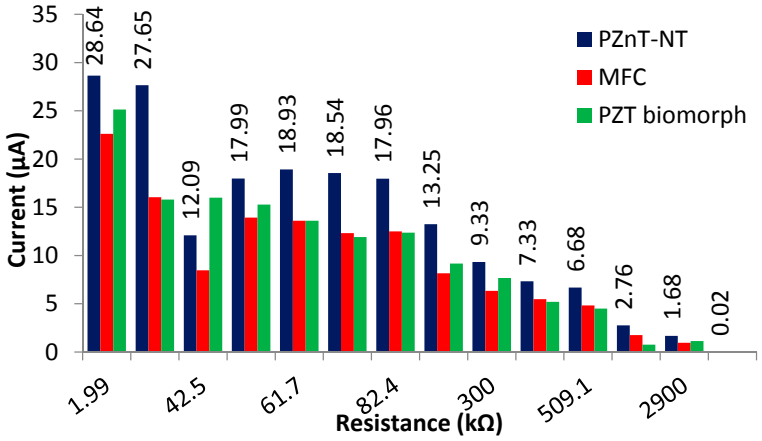

Figure 12. The generated current from the PZnT-NT, MFC, and lead zirconate titanate (PZT) bimorph.

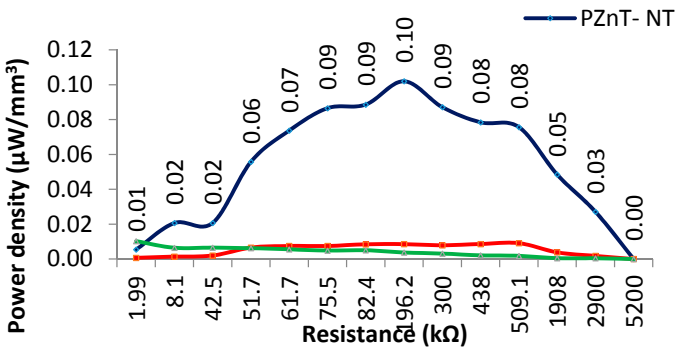

Figure 13. Power density of piezoelectric devices versus the resistance.

In general, the harvested energy level varies excessively from microwatts (μW) to milliwatts (mW); this depends on several factors, such as piezoelectric type, design of piezoelectric elements, mechanical properties, dynamic properties, electrical circuit, applied mechanical force, excitation frequency, vibration response, etc. This study focuses on the design of the piezoelectric element, which is attached to a cantilever system under low excitation frequency and low acceleration environments. The performance of the proposed harvester is compared to the results of existing research studies which implement their harvesters in a cantilever system under a similar range of excitation frequency and acceleration. The existing research works [35–42] produced a volume power density of (0.9×10^{-2}–20×10^{-2}) $\mu W/mm^3$ under the excitation frequency of (1.4–100) Hz and the acceleration of (0.2–10) ms^{-2}. The current work produces a power density of 0.10 $\mu W/mm^{-3}$ at a frequency and acceleration of 30 Hz and 0.4 ms^{-2}, respectively. Compared with other studies as recorded in Table 2, the PZnT-NT showed high sensitivity under low excitation.

Table 2. Comparison of the volume power density based on low acceleration and frequency. N/A: Not Available.

Reference	Active Material	Harvesting Technique	Active Volume (mm^3)	Acceleration/ (m/s^2)	Frequency (Hz)	Volume Power Density ($\mu W/mm^3$)
[35]	PZT bimorph	Cantilever	7040	0.2	15.00	2.69×10^{-2}
[37]	$PbZr_{0.52}Ti_{0.48}O_3$ (PZT) Flexible films	Bending and releasing	0.1	N/A	1.40	8.40×10^{-2}
[38]	PZT ceramic	Cantilever	3106	0.5	27.00	0.90×10^{-2}
[39]	MFC Flexible film	Cantilever	117.6	N/A	51.99	1.70×10^{-2}
[40]	PZT ceramic	Cantilever	≈248	0.4	38.20	18.00×10^{-2}
[41]	PZT ceramic	Cantilever	N/A	0.5–5	100.00	7.00×10^{-2}
[42]	PZT ceramic	Cantilever	588	2.0	49.70	20.00×10^{-2}
[36]	PZT ceramic	Cantilever	10.1	10.0	47.00	8.55×10^{-2}
Current work	PZnT-NT	Cantilever	300	0.4	30.00	10.00×10^{-2}

Besides PZT and MFC harvesters, the comparison between the performance of ferroelectric and non-ferroelectric nanogenerators has been shown in Table 3. It is worthwhile to mention that various figures of merit such as AC voltage (open circuit without resistance), DC voltage (close circuit with resistance), current, volume power density, or surface power density have been reported in the previous literature. So far there is no standard in selecting the figures of merit to the best knowledge of the authors. This makes the comparison difficult as most prior studies may not describe the kinematic parameters or use various figures of merit to present the harvester performance/ efficiency. To give a general overview of the harvester performance, a comparison with other existing nanogenerators using the surface power density has been made in Table 3. The existing research works produced surface power densities of (0.0006–303) $\mu W/mm^2$ under the excitation frequency of (0.5–30) Hz and the acceleration of (0.4–1.8) ms^{-2}. The current work produces a surface power density of 10 $\mu w/cm^2$ at a frequency and acceleration of 30 Hz and 0.4 ms^{-2}, respectively, which shows good progress towards building self-powered nanosystems.

Table 3. Comparison of the surface power density for numerous nanogenerators.

Reference	Materials	Polarization	Harvesting Technique	Area (cm^2)	Frequency (Hz); Acceleration (ms^{-2})	Voltage (Open Circuit) (V)	Current Density, (Short Circuit) ($\mu A/cm^2$)	Surface Power Density ($\mu W/cm^2$)
[28]	BaTiO3–PDMS	Ferroelectric	Bending and release	121	N/A	5.500	0.350	1.9000
[22]	BaTiO3-PDMS	Ferroelectric	Bending and release	0.82	N/A	1	0.190	0.1900
[43]	PMN-PT and MWCNTs	Ferroelectric	Stretchable	10	0.5 Hz; 0.817 ms^{-2}	4	0.500	0.0500
[44]	ZnSnO3/MWCNTs	Ferroelectric	Pressing by finger	11.1	N/A	40	0.036	1.0800
[6]	PZT-PDMs	Ferroelectric	Bending	0.12	N/A	6	0.380	0.1000
[45]	PbTiO3 nanotubes (PTO NTs)	Ferroelectric	Random movement induced by Wind	80×10^{-6}	N/A	0.620	0.001	0.0006
[13]	ZnO–PC100	Non-ferroelectric	Bending	0.8	N/A	1.150 *	125 *	5.6300 *
[16]	ZnO/PEDOT:PSS	Non-ferroelectric	Pressing and release	1.5	N/A	8 *	0.600 *	4.8000 *
[17]	ZnO-PCBM-P3HT	Non-ferroelectric	Bending	N/A	N/A	1.450 *	3.030 *	22.9000 *
[18]	ZnO/PEDOT:PSS	Non-ferroelectric	Bending	2	1.8 $m.s^{-2}$	0.154 *	1.580*	0.2430 *
[7]	ZnO/PMMA	Non-ferroelectric	Impact	N/A	2 Hz; 1.3 ms^{-2}	1.260	0.018	0.0226
[20]	ZnO/CuSCN/PEDOT:PSS	Non-ferroelectric	N/A	N/A	N/A	0.389 *	780 *	303 *
-	PZnT-NT (Current Work)	Non-ferroelectric	Cantilever	3	30 Hz; 0.4 ms^{-2}	N/A	N/A	10 *

* The power density was computed by using DC voltage with resistance, R = 196 kΩ.

6. Conclusions

With the aim of powering wireless sensor nodes without a battery, there is a continuous effort towards harvesting the wasted mechanical energy from low frequency and low acceleration environments, using piezoelectric materials. The ferroelectric and non-ferroelectric based piezoelectric nanogenerators are frequently examined by many researchers due to their great potential and competitive power density. In this study, a low cost non–ferroelectric $0.7PbZn_{0.3}Ti_{0.7}O_3$-$0.3Na_2TiO_3$ nanogenerator has been fabricated via a wet chemical method. The fabricated PZnT-NT harvester consisted of a ferroelectric material ($PbZn_{0.3}Ti_{0.7}O_3$) and an ion exchange material (Na_2TiO_3). $PbZn_{0.3}Ti_{0.7}O_3$ has low ferroelectric properties and low conductivity. The enhancement of the $PbZn_{0.3}Ti_{0.7}O_3$ performance has been achieved by increasing its conductivity (i.e., reducing the remnant polarization) via adding Na_2TiO_3. In this way, the permittivity can be increased which leads to power density enhancement.

The novel non-ferroelectric PZnT-NT nanogenerator demonstrated its ability to harvest the unwanted vibration energy from a vibrating cantilever beam, which was excited at a frequency and acceleration of 30 Hz and 0.4 ms^{-2}, respectively. The proposed harvester provided enough power to power an LED, which indicated a practical application of the self-powered nanosystem. Furthermore, the results showed that the PZnT-NT harvester produced the highest volume power density (i.e., 0.10 $\mu w/mm^3$), compared to the MFC (i.e., 0.014 $\mu w/mm^3$) and PZT bimorphs (i.e., 0.007 $\mu w/mm^3$). Compared to other existing nanogenerators using the surface power density, the current work produced a surface power density of 10 $\mu w/cm^2$ which verified the great potential of PZnT-NT materials in harvesting useful energy from low acceleration and low frequency environments.

In the future, it is recommended to further improve the harvester's performance via frequency tuning strategies (i.e., altering the design, dimension, and boundary conditions of the harvester in order to change its dynamic characteristics to match the excitation frequency), so that the proposed harvester is able to work in different frequency ranges. With that, the potential harvesting frequency range of the nanogenerator can be identified.

Acknowledgments: This study was supported by the Postgraduate Research Fund (PG088-2014B) and University of Malaya Research Grant (RG160-15AET). The first author wishes to express thanks to the Ministry of Higher Education and Scientific Research of Iraq for sponsoring her Ph.D. program. The suggestions and recommendations from the reviewers are gratefully acknowledged.

Author Contributions: Zainab Radeef fabricated the harvester, performed the data collection and analyses, as well as wrote the manuscript; Zainab Radeef, Chong Wen Tong, Ong Zhi Chao, and Khoo Shin Yee contributed to the conception of the study, and provided constructive suggestions for improving the study and data analyses.

Conflicts of Interest: The authors declare no conflict of interest.

References

1. EN 50324-1:2002. *Piezoelectric Properties of Ceramic Materials and Components—Part 1: Terms and Definitions*; Metrology And Testing Czech Office For Standards: Brussels, Belgium, 2002.
2. Nabunmee, S.; Taweetunkasiri; Parkpoom, J.; Rujijanagul, G. Synthesis and properties of 0.8PZT-0.10PZN-0.10PNN ceramics. *Ferroelectrics* **2011**, *416*, 22–28. [CrossRef]
3. Islam, R.A.; Priya, S. High-energy density ceramic composition in the system $Pb(Zr,Ti)O_3$–$Pb[(Zn,Ni)_{1/3}Nb_{2/3}]O_3$. *J. Am. Ceram. Soc.* **2006**, *89*, 3147–3156. [CrossRef]
4. Nogas-Ćwikiel, E. Fabrication of Mn doped PZT for ceramic-polymer composites. *Arch. Metall. Mater.* **2011**, *56*, 1065–1069. [CrossRef]
5. Kang, M.-G.; Jung, W.S.; Kang, C.Y.; Yoon, S.J. Recent progress on PZT based piezoelectric energy harvesting technologies. *Actuators* **2016**, *5*, 5. [CrossRef]
6. Wu, W.; Bai, S.; Yuan, M.; Qin, Y.; Wang, Z.L.; Jing, T. Lead zirconate titanate nanowire textile nanogenerator for wearable energy-harvesting and self-powered devices. *ACS Nano* **2012**, *6*, 6231–6235. [CrossRef] [PubMed]

7. Xu, S.; Qin, Y.; Xu, C.; Wei, Y.; Yang, R.; Wang, Z.L. Self-powered nanowire devices. *Nat. Nanotechnol.* **2010**, *5*, 366–373. [CrossRef] [PubMed]
8. Suyitno, S.; Purwanto, A.; Hidayat, R.L.L.G.; Sholahudin, I.; Yusuf, M.; Huda, S.; Arifin, Z. Fabrication and characterization of zinc oxide-based electrospun nanofibers for mechanical energy harvesting. *J. Nanotechnol. Eng. Med.* **2014**, *5*, 011002. [CrossRef]
9. Fan, F.-R.; Tian, Z.-Q.; Wang, Z. Flexible triboelectric generator. *Nano Energy* **2012**, *1*, 328–334. [CrossRef]
10. Liu, L.; Lu, K.; Wang, T.; Liao, F.; Peng, M.; Shao, M. Flexible piezoelectric nanogenerators based on silicon nanowire/α-quartz composites for mechanical energy harvesting. *Mater. Lett.* **2015**, *160*, 222–226. [CrossRef]
11. Heywang, W.; Lubitz, K.; Wersing, W. *Piezoelectricity: Evolution and Future of a Technology*; Springer-Verlag: Berlin/Heidelberg, Germany, 2008.
12. Zhu, G.; Yang, R.; Wang, S.; Wang, Z.L. Flexible high-output nanogenerator based on lateral ZnO nanowire array. *Nano Lett.* **2010**, *10*, 3151–3155. [CrossRef] [PubMed]
13. Stassi, S.; Cauda, V.; Ottone, C.; Chiodoni, A.; Pirri, C.F.; Canavese, G. Flexible piezoelectric energy nanogenerator based on ZnO nanotubes hosted in a polycarbonate membrane. *Nano Energy* **2015**, *13*, 474–481. [CrossRef]
14. Qin, W.; Li, T.; Li, Y.; Qiu, J.; Ma, X.; Chen, X.; Zhang, W. A high power ZnO thin film piezoelectric generator. *Appl. Surf. Sci.* **2016**, *364*, 670–675. [CrossRef]
15. Lee, K.Y.; Kim, D.; Lee, J.H.; Kim, T.Y.; Gupta, M.K.; Kim, S.W. Unidirectional high-power generation via stress-induced dipole alignment from $ZnSnO_3$ nanocubes/polymer hybrid piezoelectric nanogenerator. *Adv. Funct. Mater.* **2014**, *24*, 37–43. [CrossRef]
16. Lin, L.; Hu, Y.; Xu, C.; Zhang, Y.; Zhang, R.; Wen, X.; Wang, Z.L. Transparent flexible nanogenerator as self-powered sensor for transportation monitoring. *Nano Energy* **2013**, *2*, 75–81. [CrossRef]
17. Lee, K.Y.; Kumar, B.; Seo, J.S.; Kim, K.H.; Sohn, J.I.; Cha, S.N.; Kim, S.W. P-type polymer-hybridized high-performance piezoelectric nanogenerators. *Nano Lett.* **2012**, *12*, 1959–1964. [CrossRef] [PubMed]
18. Briscoe, J.; Jalali, N.; Woolliams, P.; Stewart, M.; Weaver, P.M.; Cain, M.; Dunn, S. Measurement techniques for piezoelectric nanogenerators. *Energy Environ. Sci.* **2013**, *6*, 3035–3045. [CrossRef]
19. Li, X.; Song, J.H.; Feng, S.L.; Xie, X.; Li, Z.H.; Wang, L.; Pu, Y.Y.; Soh, A.K.; Shen, J.; Lu, W.Q.; et al. High-efficiency piezoelectric micro harvester for collecting low-frequency mechanical energy. *Nanotechnology* **2016**, *27*, 485402. [CrossRef] [PubMed]
20. Jalali, N.; Briscoe, J.; Woolliams, P.; Stewart, M.; Weaver, P.M.; Cain, M.; Dunn, S. Passivation of zinc oxide nanowires for improved piezoelectric energy harvesting devices. In Journal of Physics: Conference Series (The 13th International Conference on Micro and Nanotechnology for Power Generation and Energy Conversion Applications), IOP Publishing, London, UK, 3–6 December 2013.
21. Zhang, W.; Zhu, R.; Nguyen, V.; Yang, R. Highly sensitive and flexible strain sensors based on vertical zinc oxide nanowire arrays. *Sens. Actuators A Phys.* **2014**, *205*, 164–169. [CrossRef]
22. Park, K.-I.; Xu, S.; Liu, Y.; Hwang, G.T.; Kang, S.J.L.; Wang, Z.L.; Lee, K.J. Piezoelectric $BaTiO_3$ thin film nanogenerator on plastic substrates. *Nano Lett.* **2010**, *10*, 4939–4943. [CrossRef] [PubMed]
23. Jalali, N.; Briscoe, J.; Tan, Y.Z.; Woolliams, P.; Stewart, M.; Weaver, P.M.; Dunn, S. ZnO nanorod surface modification with PDDA/PSS Bi-layer assembly for performance improvement of ZnO piezoelectric energy harvesting devices. *J. Sol. Gel Sci. Technol.* **2015**, *73*, 544–549. [CrossRef]
24. Hinchet, R.; Lee, S.; Ardila, G.; Montès, L.; Mouis, M.; Wang, Z.L. Performance optimization of vertical nanowire-based piezoelectric nanogenerators. *Adv. Funct. Mater.* **2014**, *24*, 971–977. [CrossRef]
25. Tian, S.; Wang, X. Fabrication and performances of epoxy/multi-walled carbon nanotubes/piezoelectric ceramic composites as rigid piezo-damping materials. *J. Mater. Sci.* **2008**, *43*, 4979–4987. [CrossRef]
26. Banerjee, S.; Cook-Chennault, K. An investigation into the influence of electrically conductive particle size on electromechanical coupling and effective dielectric strain coefficients in three phase composite piezoelectric polymers. *Compos. Part A Appl. Sci. Manuf.* **2012**, *43*, 1612–1619. [CrossRef]
27. Hu, S.; Shen, S.Y.; Han, H.C. Preparation and properties of PZN-PZT/PVDF piezoelectric composites modified by graphite. *Key Eng. Mater.* **2010**, *428*, 552–555. [CrossRef]
28. Park, K.I.; Lee, M.; Liu, Y.; Moon, S.; Hwang, G.T.; Zhu, G.; Lee, K.J. Flexible nanocomposite generator made of BaTiO3 nanoparticles and graphitic carbons. *Adv. Mater.* **2012**, *24*, 2999–3004. [CrossRef] [PubMed]
29. Babu, I.; De With, G. Enhanced electromechanical properties of piezoelectric thin flexible films. *Compos. Sci. Technol.* **2014**, *104*, 74–80. [CrossRef]

30. Material, Energy Harvesting from Vibration. Available online: http://www.smart-material.com/EH-product-main.html?defaulttab=2# (accessed on 15 May 2014).
31. Tichý, J.; Erhart, J.; Kittinger, E.; Prívratská, J. *Fundamentals of Piezoelectric Sensorics*; Springer: New York, NY, USA, 2010; pp. 154–156.
32. Daniels, A.; Meiling, Z.; Tiwari, A. Evaluation of piezoelectric material properties for a higher power output from energy harvesters with insight into material selection using a coupled piezoelectric-circuit-finite element method. *IEEE Trans. Ultrason. Ferroelectr. Freq. Control* **2013**, *60*, 2626–2633. [CrossRef] [PubMed]
33. Thomas, P.D.; Kunzmann, J.; Schönecker, A. *Energy Harvesting Systems Using Piezo-Electric Macro Fiber Composites*; Smart Material Corporation: Sarasota, FL, USA, 2008.
34. Amorín, H.; Correas, C.; Ramos, P.; Hungría, T.; Castro, A.; Algueró, M. Very high remnant polarization and phase-change electromechanical response of $BiFeO_3$-$PbTiO_3$ at the multiferroic morphotropic phase boundary. *Appl. Phys. Lett.* **2012**, *101*, 172908. [CrossRef]
35. Peigney, M.; Siegert, D. Piezoelectric energy harvesting from traffic-induced bridge vibrations. *Smart Mater. Struct.* **2013**, *22*, 095019. [CrossRef]
36. Liu, H.; Tay, C.J.; Quan, C.; Kobayashi, T.; Lee, C. Piezoelectric MEMS energy harvester for low-frequency vibrations with wideband operation range and steadily increased output power. *J. Microel. Syst.* **2011**, *20*, 1131–1142. [CrossRef]
37. Do, Y.H.; Jung, W.S.; Kang, M.G.; Kang, C.Y.; Yoon, S.J. Preparation on transparent flexible piezoelectric energy harvester based on PZT films by laser lift-off process. *Sens. Actuators A Phys.* **2013**, *200*, 51–55. [CrossRef]
38. Leland, E.S.; Lai, E.M.; Wright, P.K. A self-powered wireless sensor for indoor environmental monitoring. In Proceedings of the WNCG Conference, Austin, TX, USA, 20 October 2004.
39. Zhang, S.; Yan, B.; Luo, Y.; Miao, W.; Xu, M. An enhanced piezoelectric vibration energy harvesting system with macro fiber composite. *Shock Vib.* **2015**, *2015*. [CrossRef]
40. Cornwell, P.; Goethal, J.; Kowko, J.; Damianakis, M. Enhancing power harvesting using a tuned auxiliary structure. *J. Intell. Mater. Syst. Struct.* **2005**, *16*, 825–834. [CrossRef]
41. Roundy, S.; Wright, P.K.; Rabaey, J. A study of low level vibrations as a power source for wireless sensor nodes. *Comput. Commun.* **2003**, *26*, 1131–1144. [CrossRef]
42. Berdy, D.F.; Srisungsitthisunti, P.; Jung, B.; Xu, X.; Rhoads, J.F.; Peroulis, D. Low-frequency meandering piezoelectric vibration energy harvester. *IEEE Trans. Ultrason. Ferroelectr. Freq. Control* **2012**, *59*, 846–858. [CrossRef] [PubMed]
43. Lee, J.; Han, S.; Ryu, J.; Hwang, G.T.; Park, D.Y.; Park, J.H.; Lee, S.S.; Byun, M.; Ko, S.H.; Lee, K.J. A hyper-stretchable elastic-composite energy harvester. *Adv. Mater.* **2015**, *27*, 2866–2875.
44. Alam, M.M.; Ghosh, S.K.; Sultana, A.; Mandal, D. Lead-free $ZnSnO_3$/MWCNTs-based self-poled flexible hybrid nanogenerator for piezoelectric power generation. *Nanotechnology* **2015**, *26*, 165403. [CrossRef] [PubMed]
45. Lee, Y.B.; Han, J.K.; Noothongkaew, S.; Kim, S.K.; Song, W.; Myung, S.; Lee, S.S.; Lim, J.; Bu, S.D.; An, K.S. Toward arbitrary-direction energy harvesting through flexible piezoelectric nanogenerators using perovskite $PbTiO_3$ nanotube arrays. *Adv. Mater.* **2017**, *29*. [CrossRef] [PubMed]